Measurement of lepton momentum moments in the decay $\bar{B} \to X\ell\bar{\nu}$ and determination of the heavy quark expansion parameters and $|V_{cb}|$

A. H. Mahmood,[1] S. E. Csorna,[2] I. Danko,[2] G. Bonvicini,[3] D. Cinabro,[3] M. Dubrovin,[3] S. McGee,[3] A. Bornheim,[4]
E. Lipeles,[4] S. P. Pappas,[4] A. Shapiro,[4] W. M. Sun,[4] A. J. Weinstein,[4] R. A. Briere,[5] G. P. Chen,[5] T. Ferguson,[5] G. Tatishvili,[5]
H. Vogel,[5] N. E. Adam,[6] J. P. Alexander,[6] K. Berkelman,[6] V. Boisvert,[6] D. G. Cassel,[6] P. S. Drell,[6] J. E. Duboscq,[6]
K. M. Ecklund,[6] R. Ehrlich,[6] R. S. Galik,[6] L. Gibbons,[6] B. Gittelman,[6] S. W. Gray,[6] D. L. Hartill,[6] B. K. Heltsley,[6] L. Hsu,[6]
C. D. Jones,[6] J. Kandaswamy,[6] D. L. Kreinick,[6] A. Magerkurth,[6] H. Mahlke-Krüger,[6] T. O. Meyer,[6] N. B. Mistry,[6]
J. R. Patterson,[6] D. Peterson,[6] J. Pivarski,[6] S. J. Richichi,[6] D. Riley,[6] A. J. Sadoff,[6] H. Schwarthoff,[6] M. R. Shepherd,[6]
J. G. Thayer,[6] D. Urner,[6] T. Wilksen,[6] A. Warburton,[6] M. Weinberger,[6] S. B. Athar,[7] P. Avery,[7] L. Breva-Newell,[7] V. Potlia,[7]
H. Stoeck,[7] J. Yelton,[7] K. Benslama,[8] B. I. Eisenstein,[8] G. D. Gollin,[8] I. Karliner,[8] N. Lowrey,[8] C. Plager,[8] C. Sedlack,[8]
M. Selen,[8] J. J. Thaler,[8] J. Williams,[8] K. W. Edwards,[9] R. Ammar,[10] D. Besson,[10] X. Zhao,[10] S. Anderson,[11]
V. V. Frolov,[11] D. T. Gong,[11] Y. Kubota,[11] S. Z. Li,[11] R. Poling,[11] A. Smith,[11] C. J. Stepaniak,[11] J. Urheim,[11] Z. Metreveli,[12]
K. K. Seth,[12] A. Tomaradze,[12] P. Zweber,[12] S. Ahmed,[13] M. S. Alam,[13] J. Ernst,[13] L. Jian,[13] M. Saleem,[13] F. Wappler,[13]
K. Arms,[14] E. Eckhart,[14] K. K. Gan,[14] C. Gwon,[14] K. Honscheid,[14] D. Hufnagel,[14] H. Kagan,[14] R. Kass,[14] T. K. Pedlar,[14]
E. von Toerne,[14] M. M. Zoeller,[14] H. Severini,[15] P. Skubic,[15] S. A. Dytman,[16] J. A. Mueller,[16] S. Nam,[16] V. Savinov,[16]
S. Chen,[17] J. W. Hinson,[17] J. Lee,[17] D. H. Miller,[17] V. Pavlunin,[17] E. I. Shibata,[17] I. P. J. Shipsey,[17] D. Cronin-Hennessy,[18]
A. L. Lyon,[18] C. S. Park,[18] W. Park,[18] J. B. Thayer,[18] E. H. Thorndike,[18] T. E. Coan,[19] Y. S. Gao,[19] F. Liu,[19]
Y. Maravin,[19] R. Stroynowski,[19] M. Artuso,[20] C. Boulahouache,[20] S. Blusk,[20] K. Bukin,[20] E. Dambasuren,[20] R. Mountain,[20]
H. Muramatsu,[20] R. Nandakumar,[20] T. Skwarnicki,[20] S. Stone,[20] and J. C. Wang[20]

(CLEO Collaboration)

[1]*University of Texas–Pan American, Edinburg, Texas 78539*
[2]*Vanderbilt University, Nashville, Tennessee 37235*
[3]*Wayne State University, Detroit, Michigan 48202*
[4]*California Institute of Technology, Pasadena, California 91125*
[5]*Carnegie Mellon University, Pittsburgh, Pennsylvania 15213*
[6]*Cornell University, Ithaca, New York 14853*
[7]*University of Florida, Gainesville, Florida 32611*
[8]*University of Illinois, Urbana-Champaign, Illinois 61801*
[9]*Carleton University, Ottawa, Ontario, Canada K1S 5B6*
and the Institute of Particle Physics, Canada M5S 1A7
[10]*University of Kansas, Lawrence, Kansas 66045*
[11]*University of Minnesota, Minneapolis, Minnesota 55455*
[12]*Northwestern University, Evanston, Illinois 60208*
[13]*State University of New York at Albany, Albany, New York 12222*
[14]*Ohio State University, Columbus, Ohio 43210*
[15]*University of Oklahoma, Norman, Oklahoma 73019*
[16]*University of Pittsburgh, Pittsburgh, Pennsylvania 15260*
[17]*Purdue University, West Lafayette, Indiana 47907*
[18]*University of Rochester, Rochester, New York 14627*
[19]*Southern Methodist University, Dallas, Texas 75275*
[20]*Syracuse University, Syracuse, New York 13244*

We measure the primary lepton momentum spectrum in $\bar{B} \to X\ell\bar{\nu}$ decays, for $p_\ell \geq 1.5$ GeV/c in the B rest frame. From this, we calculate various moments of the spectrum. In particular, we find $R_0 \equiv \int_{1.7 \text{ GeV}} (d\Gamma/dE_{sl}) dE_\ell / \int_{1.5 \text{ GeV}} (d\Gamma/dE_{sl}) dE_\ell = 0.6187 \pm 0.0014_{stat} \pm 0.0016_{sys}$ and $R_1 \equiv \int_{1.5 \text{ GeV}} E_\ell (d\Gamma/dE_{sl}) dE_\ell / \int_{1.5 \text{ GeV}} (d\Gamma/dE_{sl}) dE_\ell = (1.7810 \pm 0.0007_{stat} \pm 0.0009_{sys})$ GeV. We use these moments to determine non-perturbative parameters governing the semileptonic width. In particular, we extract the heavy quark expansion parameters $\bar{\Lambda} = (0.39 \pm 0.03_{stat} \pm 0.06_{sys} \pm 0.12_{th})$ GeV and $\lambda_1 = (-0.25 \pm 0.02_{stat} \pm 0.05_{sys} \pm 0.14_{th})$ GeV^2. The theoretical constraints used are evaluated through order $1/M_B^3$ in the non-perturbative expansion and $\beta_0 \alpha_s^2$ in the perturbative expansion. We use these parameters to extract $|V_{cb}|$ from the world average of the semileptonic width and find $|V_{cb}| = (40.8 \pm 0.5_{\Gamma_{sl}} \pm 0.4_{(\lambda_1, \bar{\Lambda})_{exp}} \pm 0.9_{th}) \times 10^{-3}$. In addition, we extract the short range b-quark mass $m_b^{1S} = (4.82 \pm 0.07_{exp} \pm 0.11_{th})$ GeV/c^2. Finally, we discuss the implications of our measurements for the theoretical understanding of inclusive semileptonic processes.

I. INTRODUCTION

Experimental data on inclusive B meson semileptonic decays can in principle provide a very precise method to determine the Cabibbo-Kobayashi-Maskawa (CKM) quark mixing parameter $|V_{cb}|$ [1]. A crucial theoretical input is the hadronic matrix element needed to express the measured semileptonic width in terms of $|V_{cb}|$. Heavy quark expansion (HQE) [2–5] is a QCD-based approach to inclusive processes that casts perturbative and non-perturbative corrections to the partonic width as power series expansions. An underlying assumption of this approach is quark-hadron duality. It is important to quantify the uncertainties induced by the neglected higher order terms in the non-perturbative expansion, as well as the uncertainty introduced by possible duality violations, in order to achieve a full understanding of the theoretical errors and be able to ascertain the true uncertainty on $|V_{cb}|$. The only strategy proposed so far to gather further insight is to measure several quantities predicted in this framework. A precise measurement of the lepton spectrum is an important element of this program and is the key result presented in this paper.

The theoretical expression for the inclusive semileptonic width for $\bar{B} \to X \ell \bar{\nu}$ ($\ell = \mu$ or e) through $\mathcal{O}(1/M_B^3)$ in the non-perturbative expansion and $\beta_0(\alpha_s/\pi)^2$ in the perturbative one is given by [4,6]

$$
\begin{aligned}
\Gamma_{sl} = \frac{G_F^2 |V_{cb}|^2 M_B^5}{192\pi^3} \; 0.3689 \Bigg[& 1 - 1.54\frac{\alpha_s}{\pi} - 1.43\beta_0\left(\frac{\alpha_s}{\pi}\right)^2 \\
& - 1.648\frac{\bar{\Lambda}}{M_B}\left(1 - 0.87\frac{\alpha_s}{\pi}\right) - 0.946\left(\frac{\bar{\Lambda}}{M_B}\right)^2 - 3.185\frac{\lambda_1}{M_B^2} \\
& + 0.02\frac{\lambda_2}{M_B^2} - 0.298\left(\frac{\bar{\Lambda}}{M_B}\right)^3 - 3.28\frac{\lambda_1\bar{\Lambda}}{M_B^3} + 10.47\frac{\lambda_2\bar{\Lambda}}{M_B^3} \\
& - 6.153\frac{\rho_1}{M_B^3} + 7.482\frac{\rho_2}{M_B^3} - 7.4\frac{\tau_1}{M_B^3} + 1.491\frac{\tau_2}{M_B^3} \\
& - 10.41\frac{\tau_3}{M_B^3} - 7.482\frac{\tau_4}{M_B^3} + \mathcal{O}\left(\frac{1}{M_B^4}\right) \Bigg],
\end{aligned} \tag{1}
$$

where $\beta_0 = (33 - 2n_f)/3 = 25/3$ is the one-loop QCD beta function and n_f is the number of relevant flavors and the form factors ρ_1, ρ_2, τ_1, τ_2, τ_3, and τ_4 are the parameters of the $1/M_B^3$ terms in the non-perturbative expansion. These $1/M_B^3$ form factors are expected, from dimensional arguments, to be of the order Λ_{QCD}^3, and thus they are generally assumed to be $\leq (0.5)^3$ GeV^3. In addition, ρ_1 is expected to be positive from the vacuum-saturation approximation [7]. Furthermore, as Gremm and Kapustin have noted [4], the $B^\star - B$ and $D^\star - D$ mass splittings impose the constraint

$$\rho_2 - \tau_2 - \tau_4$$

$$= \frac{\kappa(m_c)M_B^2\Delta M_B(M_D + \bar{\Lambda}) - M_D^2\Delta M_D(m_B + \bar{\Lambda})}{M_B + \bar{\Lambda} - \kappa(m_c)(M_D + \bar{\Lambda})}, \tag{2}$$

where m_b and m_c represent the beauty and charm quark masses, respectively; $\kappa(m_c) \equiv [\alpha_s(m_c)/\alpha_s(m_b)]^{(3/\beta_0)}$ and $\Delta M_B(\Delta M_D)$ represents the vector-pseudoscalar meson splitting in the beauty (charm) sector.

The parameter λ_1 [2,3] is related to the expectation value of the operator corresponding to the kinetic energy of the b quark inside the B meson:

$$\lambda_1 = \frac{1}{2M_B}\langle B(v)|\bar{h}_v(iD)^2 h_v|B(v)\rangle, \tag{3}$$

where v denotes the 4-velocity of the heavy hadron and h_v is the quark field in the heavy quark effective theory. The parameter λ_2 [2,3] is the expectation value of the leading chromomagnetic operator that breaks the heavy quark spin symmetry. It is formally defined as

$$\lambda_2 = \frac{-1}{2M_B}\left\langle B(v)\left|\bar{h}_v\frac{g}{2}\cdot\sigma^{\mu\nu}G_{\mu\nu}h_v\right|B(v)\right\rangle, \tag{4}$$

where h_v is the heavy quark field and $|B(v)\rangle$ is the B meson state. The value of λ_2 is determined from the $B^\star - B$ mass difference to be 0.128 ± 0.010 GeV^2. The quantity $\bar{\Lambda}$ is related to the b-quark pole mass m_b [2,3] through the expression

$$m_b = \bar{M}_B - \bar{\Lambda} + \frac{\lambda_1}{2m_b}, \tag{5}$$

where $\bar{M}_B$ is the spin-averaged $B^{(\star)}$ mass ($\bar{M}_B = 5.313$ GeV/c^2). A similar relationship holds between the c-quark mass m_c and the spin-averaged charm meson mass ($\bar{M}_D = 1.975$ GeV/c^2).

The shape of the lepton momentum spectrum in $\bar{B} \to X \ell \bar{\nu}$ decays can be used to measure the HQE parameters λ_1 and $\bar{\Lambda}$, through its energy moments, which are also predicted in the heavy quark expansion. We choose to study truncated moments of the lepton spectrum, with a momentum cut of $p_\ell \geq 1.5$ GeV/c in the B meson rest frame. This choice decreases the sensitivity of our measurement to the secondary leptons from the cascade decays ($b \to c \to s\ell\nu$ or $d\ell\nu$).

We extract the HQE parameters $\bar{\Lambda}$ and λ_1 from measurements of two moments originally suggested by Gremm *et al.*[1]:

$$R_0 = \frac{\displaystyle\int_{1.7 \text{ GeV}} (d\Gamma_{sl}/dE_\ell)dE_\ell}{\displaystyle\int_{1.5 \text{ GeV}} (d\Gamma_{sl}/dE_\ell)dE_\ell} \tag{6}$$

and

---

[1] Our notation is different than that used in Ref. [8], where R_0 is first introduced as R_2.

$$R_1 = \frac{\int_{1.5 \text{ GeV}} E_\ell (d\Gamma_{sl}/dE_\ell) dE_\ell}{\int_{1.5 \text{ GeV}} (d\Gamma_{sl}/dE_\ell) dE_\ell}. \qquad (7)$$

The integration interval in the numerator of these expressions is chosen to be large enough to make a comparison between the HQE predictions and experimental data relevant [8]. The theoretical expressions for these moments $R_{0,1}^{th}$ [4,9] are evaluated by integrating the dominant $b \to c\ell\bar{\nu}$ component of the lepton spectrum. In addition, the small contribution coming from charmless semileptonic decays $b \to u\ell\bar{\nu}$ is included by adding the contribution from $d\Gamma_u/dE_\ell$, scaled by $|V_{ub}/V_{cb}|^2$ [8,9].

We determine these two moments from the measured lepton spectrum in $\bar{B} \to X\ell\bar{\nu}$ and insert them in the theoretical expressions to extract the two parameters λ_1 and $\bar{\Lambda}$. We have previously published experimental determinations of $\bar{\Lambda}$ and λ_1 obtained by studying the E_γ spectrum in $b \to s\gamma$ [10] and the first moment of the mass M_X of the hadronic system recoiling against the $\ell\bar{\nu}$ pair in $\bar{B} \to X\ell\bar{\nu}$ decays [11]. We compare our results to these measurements.

In recent years, increasing attention has been focused on "short-range masses," preferred by some authors as they are not affected by renormalon ambiguities [12]. In particular, the so-called 1S b-quark mass, m_b^{1S}, defined as one-half of the energy of the 1S $b\bar{b}$ state calculated in perturbation theory, has been extracted from $\Upsilon(1S)$ resonance data [13]. The mass m_b^{1S} has been shown to have remarkably well-behaved perturbative relations to other physical quantities such as the hadronic matrix element governing the $b \to u$ semileptonic width [14]. Using the formalism developed by Bauer and Trott [9], we have used the spectral moments R_0 and R_1 to determine m_b^{1S}.

These authors also explore different lepton energy moments, by varying the exponent of the energy in the integrands and the lower limits of integration. In particular, they identify several moments that provide constraints for m_b^{1S} and λ_1 that are less sensitive to higher order terms in the non-perturbative expansion. We study four such moments defined as

$$R_a^{(3)} = \frac{\int_{1.7 \text{ GeV}} E_\ell^{0.7} (d\Gamma_{sl}/dE_\ell) dE_\ell}{\int_{1.5 \text{ GeV}} E_\ell^2 (d\Gamma_{sl}/dE_\ell) dE_\ell}, \qquad (8)$$

$$R_b^{(3)} = \frac{\int_{1.6 \text{ GeV}} E_\ell^{0.9} (d\Gamma_{sl}/dE_\ell) dE_\ell}{\int_{1.7 \text{ GeV}} (d\Gamma_{sl}/dE_\ell) dE_\ell}, \qquad (9)$$

$$R_a^{(4)} = \frac{\int_{1.6 \text{ GeV}} E_\ell^{0.8} (d\Gamma_{sl}/dE_\ell) dE_\ell}{\int_{1.7 \text{ GeV}} (d\Gamma_{sl}/dE_\ell) dE_\ell}, \qquad (10)$$

and

$$R_b^{(4)} = \frac{\int_{1.6 \text{ GeV}} E_\ell^{2.5} (d\Gamma_{sl}/dE_\ell) dE_\ell}{\int_{1.5 \text{ GeV}} E_\ell^{2.9} (d\Gamma_{sl}/dE_\ell) dE_\ell}. \qquad (11)$$

The values of $\bar{\Lambda}$ and λ_1 determined with the latter set of constraints have different relative weights of the experimental and theoretical uncertainties and thus provide complementary information.

Finally, Bauer and Trott identify moments that are insensitive to m_b^{1S} and λ_1. They suggest that a comparison between theoretical evaluations of these "duality moments" and their experimental values may provide useful constraints on possible quark-hadron duality violations in semileptonic processes. We report our measurement of two such "duality moments," defined as

$$D_3 = \frac{\int_{1.6 \text{ GeV}} E_\ell^{0.7} (d\Gamma_{sl}/dE_\ell) dE_\ell}{\int_{1.5 \text{ GeV}} E_\ell^{1.5} (d\Gamma_{sl}/dE_\ell) dE_\ell} \qquad (12)$$

and

$$D_4 = \frac{\int_{1.6 \text{ GeV}} E_\ell^{2.3} (d\Gamma_{sl}/dE_\ell) dE_\ell}{\int_{1.5 \text{ GeV}} E_\ell^{2.9} (d\Gamma_{sl}/dE_\ell) dE_\ell}. \qquad (13)$$

This measurement, together with new emerging experimental information on a variety of moments of the kinematic observables in b semileptonic decays [15,16], may eventually lead to a more complete assessment of our present understanding of inclusive semileptonic decays.

II. EXPERIMENTAL METHOD

The data sample used in this study was collected with the CLEO II detector [17] at the CESR e^+e^- collider. It consists of an integrated luminosity of 3.14 fb^{-1} at the $\Upsilon(4S)$ energy, corresponding to a sample of 3.3×10^6 $B\bar{B}$ events. The continuum background is studied with a sample of 1.61 fb^{-1} collected at an energy about 60 MeV below the resonance.

We measure the momentum spectrum of electrons and muons with a minimum momentum of 1.5 GeV/c in the B meson center-of-mass frame. This momentum requirement ensures good efficiency and background rejection for both lepton species, thereby allowing us to check systematic ef-
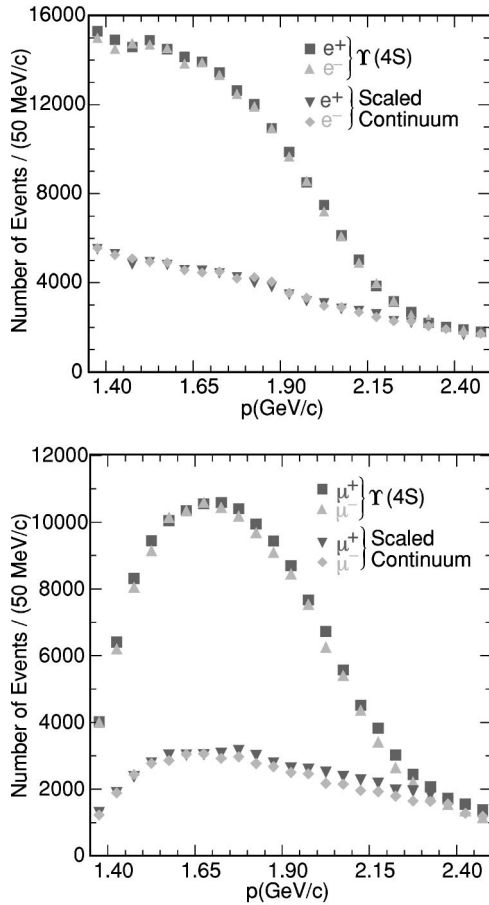
FIG. 1. Raw lepton momentum spectra from the $\Upsilon(4S)$ and scaled continuum.

FIG. 2. Background components of the electron (top) and muon (bottom) momentum spectra from processes (π^0 decays and γ conversion for electrons only, and J/Ψ decays and fakes for both leptons) that are estimated with data.

fects with the μ/e ratio. For muons we have adequate efficiency and background rejection only above $p_\mu \sim 1.3$ GeV/c. In addition, in this range the inclusive spectra are dominated by the direct $b \to c \ell \nu$ semileptonic decay, with only a small contamination by secondary leptons produced in the decay chain $b \to c \to (s \ell \nu$ or $d \ell \nu)$.

Electrons are identified with a likelihood method that includes several discriminating variables, most importantly the ratio E/p of the energy deposited in the electromagnetic calorimeter to the reconstructed momentum, and the specific ionization in the central drift chamber. Muon candidates are required to penetrate at least five nuclear interaction lengths of absorber material. We use the central part of the detector ($|\cos\theta| \leq 0.71$ for electrons and $|\cos\theta| \leq 0.61$ for muons).

The overall efficiency is the product of three factors: the reconstruction efficiency, including event selection criteria and acceptance corrections; the tracking efficiency; and the μ or e identification efficiency. The first two factors are estimated with Monte Carlo simulations and checked with data, whereas the lepton identification efficiencies are studied with data: radiative μ-pair events for the μ efficiency and radiative Bhabha electron tracks embedded in hadronic events for the e efficiency. The e identification efficiency is nearly constant in our momentum range and equal to (93.8 ± 2.6)%. The μ momentum threshold is near our low mo-
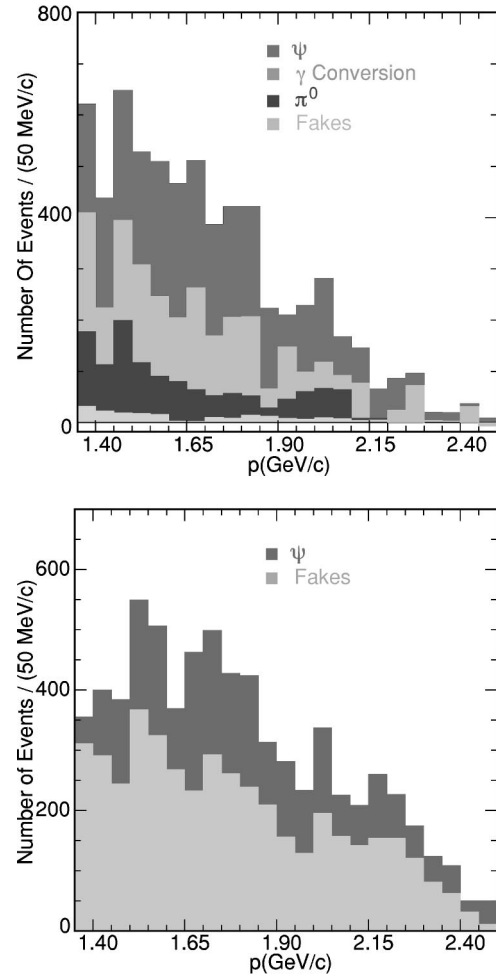
mentum cut, and the efficiency rises to a plateau of about 95% above 2.0 GeV/c. The distortion in momentum induced by radiation emitted in the detector and other instrumental effects is corrected for by using the same Monte Carlo samples used in the efficiency correction.

Figure 1 shows the raw yields for electrons (top) and muons (bottom) from the $\Upsilon(4S)$ sample and the continuum background. The latter is estimated from scaled off-resonance data. The scaling factor for the continuum sample is determined by the ratio of integrated luminosities and continuum cross sections and is 1.930 ± 0.013. This scale factor has been determined independently using tracks with momenta higher than the kinematic limit for B-meson decay products. In all the cases no statistically significant lepton yield has been observed beyond the end point for B decays, within errors. The study of these control samples is used to determine the systematic error on the continuum scale factor.

The raw yields include hadrons misidentified as leptons (fakes). This contribution is determined from data as follows. Fake rates are determined from tagged samples: charged pions from $K_S^0 \to \pi^+ \pi^-$, charged kaons from $D^{\star+}$
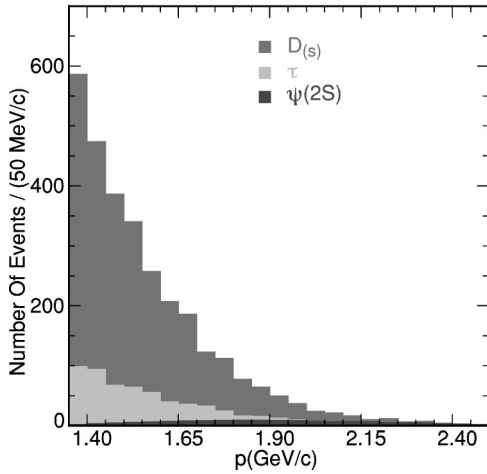
FIG. 3. Background components of the electron momentum spectrum that are studied with Monte Carlo simulations; these components are similar in the muon case.
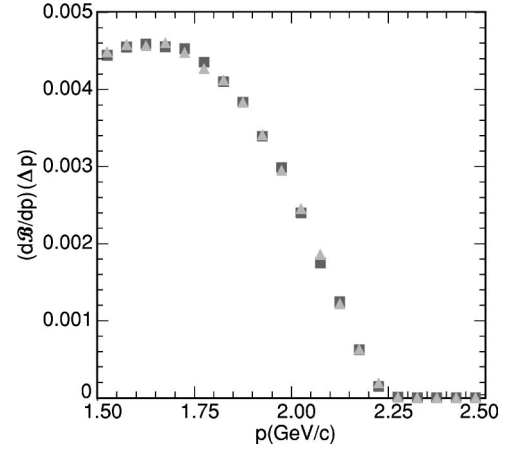

FIG. 4. Corrected electron (triangles) and muon (squares) momentum spectra in the B-meson rest frame, where $d\mathcal{B}$ represents the differential semileptonic branching fraction in the bin Δp, divided by the number of B mesons in the sample.

$\to D^0 \pi^+, D^0 \to K^- \pi^+$, and protons from $\Lambda \to p \pi^-$. The momentum-dependent probability for misidentifying a hadron track as an electron or muon is then determined by weighting the pion, kaon, and proton probabilities according to particle abundances determined with $B\bar{B}$ Monte Carlo. The fake correction applied to the data is obtained by folding these fake probabilities with the measured spectra of hadronic tracks in $B\bar{B}$ events.

We correct for several sources of real leptons. Leptons from J/ψ decays are vetoed by combining a candidate with another lepton of the same type and opposite sign and removing it if their invariant mass is within 3σ of the known J/ψ mass. A correction is made for veto inefficiency. A similar procedure is applied to electrons and positrons coming from π^0 Dalitz decays and from γ conversions.

Finally, we subtract leptons coming from $\psi(2S)$ decays or the secondary decays $b \to c \to (s\ell\nu$ or $d\ell\nu)$ and $B \to \tau \to \ell\nu\bar{\nu}$ using Monte Carlo simulations. Figures 2 and 3 show the individual estimated background contributions to our sample. Note that all of the backgrounds are small compared to the signal.

Our goal is a precise determination of the shape of the lepton momentum spectrum, so corrections for the distortion introduced by electroweak radiative effects are important. We use the prescription developed by Atwood and Marciano [18]. This procedure incorporates leading-logarithm and short-distance loop corrections, and sums soft-virtual and real-photon corrections to all orders. It does not incorporate hard-photon bremsstrahlung, which mainly modifies the low energy portion of the electron spectrum, and is not used in our analysis. An independent method of studying QED radiative corrections in semileptonic decays, based on the simulation package PHOTOS [19], has been used to obtain an independent assessment of the corrections. The difference between the two methods is used to obtain the systematic error of this correction.

Finally, we use a Monte Carlo sample of $b \to c\ell\bar{\nu}$ events to derive a matrix to unfold the corrected spectra from the

laboratory frame into the B-meson rest frame. [B mesons produced at the $\Upsilon(4S)$ by the Cornell Electron Storage Ring (CESR) e^+e^- collider typically have a momentum of $p_B \sim 300$ MeV/c in the laboratory frame.] Our lower momentum limit of 1.35 GeV/c for the measurement of the lepton spectra ensures that end effects in the unfolding procedure do not introduce distortions into the determination of the spectral moments. The measured spectrum includes leptons from $b \to c\ell\bar{\nu}$ and $b \to u\ell\bar{\nu}$. Figure 4 shows the resulting electron and muon spectra. While the curves shown combine both signs of lepton charges, we have also studied positive and negative leptons separately and found good agreement between them. Although the $b \to u\ell\bar{\nu}$ tail beyond the end point of charmed semileptonic decay is not shown in Fig. 4, this component of the charmless semileptonic spectrum is unfolded and added separately to the measured moments.

Our first step is the determination of the truncated moments R_0 and R_1 defined in Eqs. (6) and (7), respectively. Using the measured spectra, we evaluate the relevant integrals and obtain the results shown in Table I, where the first error is statistical and the second is systematic in each quoted number. Table II summarizes our studies of several sources of systematic uncertainty and their effect on the moments R_0 and R_1. The dominant uncertainty for both lepton species is related to particle identification efficiency. As the moments are ratios of measured quantities, the effects of several uncertainties, which are nearly independent of the lepton energy, cancel. The overall systematic uncertainties are 0.28% for R_0^{exp} and 0.06% for R_1^{exp} for the $e^\pm$ sample, and 0.32%

TABLE I. Measured truncated lepton moments for $e^\pm \mu^\pm$ and combined (weighted average of $e^\pm$ and $\mu^\pm$).

	R_0^{exp}	R_1^{exp} (GeV)
$e^\pm$	$0.6184 \pm 0.0016 \pm 0.0017$	$1.7817 \pm 0.0008 \pm 0.0010$
$\mu^\pm$	$0.6189 \pm 0.0023 \pm 0.0020$	$1.7802 \pm 0.0011 \pm 0.0011$
$\ell^\pm$	$0.6187 \pm 0.0014 \pm 0.0016$	$1.7810 \pm 0.0007 \pm 0.0009$

TABLE II. Summary of the statistical and systematic errors on the moments R_0^{exp} and R_1^{exp}.

	$\delta R_0 (\times 10^3)$		$\delta R_1 (\text{GeV})(\times 10^3)$	
	$e^\pm$	$\mu^\pm$	$e^\pm$	$\mu^\pm$
Statistical error	1.6	2.3	0.8	1.1
Continuum subtraction	0.42	0.30	0.36	0.27
J/ψ veto	0.15	0.07	0.10	0.08
π^0 veto	0.04	N/A	0.01	N/A
Leptons from $b \to c \to s(d) \ell \nu$	0.64	0.70	0.20	0.30
Leptons from $B \to \tau X$	0.22	0.25	0.10	0.10
Fake leptons	0.04	0.02	0.02	0.19
Detection efficiency	0.10	0.08	0.20	0.08
Particle identification efficiency	0.91	1.52	0.40	0.65
Electroweak radiative correction	0.75	0.43	0.25	0.15
$B \to X_u \ell \bar{\nu}$ shape uncertainty	0.50	0.40	0.40	0.30
Unfolding effect	0.34	0.44	0.14	0.12
Absolute momentum scale uncert.	0.70	0.70	0.50	0.50
Total systematic uncertainties	1.7	2.0	1.0	1.1

and 0.06% for the $\mu^\pm$ sample. These are comparable to the statistical uncertainties. Since the two moments are extracted from the same spectra, we must use the covariance matrix $E_{R_0 R_1}$ to extract the HQE parameters. Table III shows the numerical values of the $E_{R_0 R_1}$ elements for electrons and muons.

III. DETERMINATION OF THE HQE PARAMETERS

First, we determine $\bar{\Lambda}$ and λ_1 using the published expressions for the moments R_0 and R_1 in terms of the HQE parameters [8]. In addition, we explore the implications of other constraints derived from the lepton energy spectrum [9].

A. Determination of $\bar{\Lambda}$ and λ_1 from the moments R_0 and R_1

The theoretical expressions [8,9] relating the spectral moments to the HQE parameters include correction terms accounting for electroweak radiative effects and the unfolding from the laboratory to the rest frame. We do not use these

TABLE III. Covariance matrices for the experimental errors on R_0^{exp} and R_1^{exp} moments.

	$E_{R_0 R_1} (\times 10^6)$
$e^\pm$	$\begin{pmatrix} 5.5 & 1.1 \\ 1.1 & 1.6 \end{pmatrix}$
$\mu^\pm$	$\begin{pmatrix} 5.2 & 2.2 \\ 2.2 & 9.3 \end{pmatrix}$
$\ell^\pm$	$\begin{pmatrix} 4.5 & 0.8 \\ 0.8 & 1.3 \end{pmatrix}$

additional terms because our data are corrected for these effects. The non-perturbative expansion [2–4] includes terms through order $1/M_B^3$.

The values of the HQE parameters and their experimental uncertainties are obtained by calculating the χ^2 from the measured moments R_0^{exp} and R_1^{exp} and the covariance matrix $E_{R_0 R_1}$

$$\chi^2 = \sum_{\alpha=0}^{\alpha=1} \sum_{\beta=0}^{\beta=1} (R_\alpha^{exp} - R_\alpha^{th}) E_{R_0 R_1}^{-1} (R_\beta^{exp} - R_\beta^{th}), \quad (14)$$

where R_0^{th} and R_1^{th} are

$$R_0^{th} = 0.6581 - 0.315 \left(\frac{\bar{\Lambda}}{\bar{M}_B} \right) - 0.68 \left(\frac{\bar{\Lambda}}{\bar{M}_B} \right)^2 - 1.65 \left(\frac{\lambda_1}{\bar{M}_B^2} \right)$$

$$- 4.94 \left(\frac{\lambda_2}{\bar{M}_B^2} \right) + \left| \frac{V_{ub}}{V_{cb}} \right|^2 \left(0.87 - 3.8 \frac{\bar{\Lambda}}{\bar{M}_B} \right) - 1.5 \left(\frac{\bar{\Lambda}}{\bar{M}_B} \right)^3$$

$$- 7.1 \left(\frac{\bar{\Lambda}\lambda_1}{\bar{M}_B^3} \right) - 17.1 \left(\frac{\bar{\Lambda}\lambda_2}{\bar{M}_B^3} \right) - 1.8 \left(\frac{\rho_1}{\bar{M}_B^3} \right) + 2.3 \left(\frac{\rho_2}{\bar{M}_B^3} \right)$$

$$- 2.9 \left(\frac{\tau_1}{\bar{M}_B^3} \right) - 1.5 \left(\frac{\tau_2}{\bar{M}_B^3} \right) - 4.0 \left(\frac{\tau_3}{\bar{M}_B^3} \right) - 4.9 \left(\frac{\tau_4}{\bar{M}_B^3} \right)$$

$$- \frac{\alpha_s}{\pi} \left(0.039 + 0.18 \frac{\bar{\Lambda}}{\bar{M}_B} \right) - 0.098 \left(\frac{\alpha_s}{\pi} \right)^2 \beta_0 \quad (15)$$
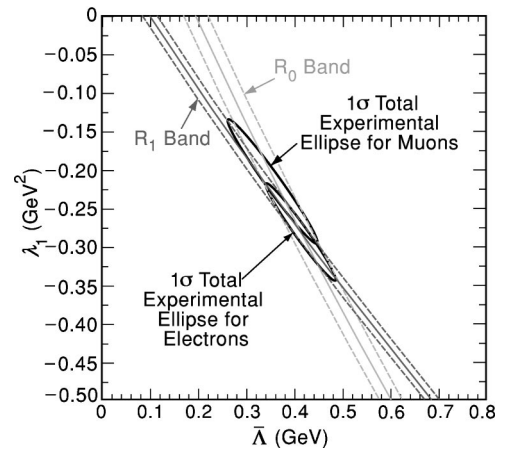
FIG. 5. Constraints on the HQE parameters λ_1 and $\bar{\Lambda}$ from our measured moments of the electron and muon momentum spectra R_0 and R_1. The contours represent $\Delta \chi^2 = 1$ for the combined statistical and systematic errors on the measured values. The parameters λ_1 and $\bar{\Lambda}$ are computed in the $\overline{\text{MS}}$ scheme to order $1/M_B^3$ and $\beta_0 \alpha_s^2$.
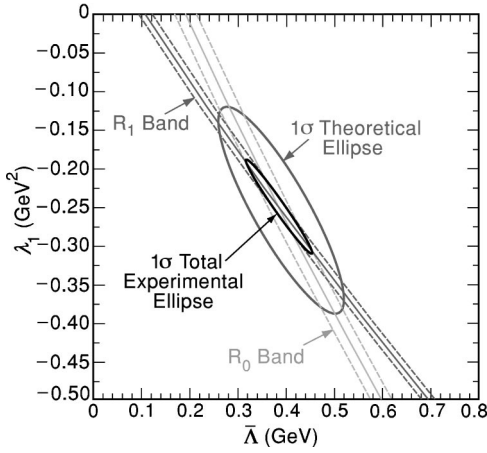
FIG. 6. The constraints from our combined electron and muon R_0 and R_1 moments, with $\Delta\chi^2 = 1$ contours for total experimental and theoretical uncertainties. The parameters λ_1 and $\bar{\Lambda}$ are computed in the $\overline{\mathrm{MS}}$ scheme to order $1/M_B^3$ and $\beta_0\alpha_s^2$.

FIG. 7. Experimental constraints from the $\bar{B} \to X\ell\bar{\nu}$ hadronic mass moment and $b \to s\gamma$ E_γ moment [11] compared with the combined electron and muon R_0 and R_1 constraints. The parameters λ_1 and $\bar{\Lambda}$ are computed in the $\overline{\mathrm{MS}}$ scheme to order $1/M_B^3$ and $\beta_0\alpha_s^2$.

and

$$R_1^{th} = 1.8059 - 0.309\left(\frac{\bar{\Lambda}}{\bar{M}_B}\right) - 0.35\left(\frac{\bar{\Lambda}}{\bar{M}_B}\right)^2 - 2.32\left(\frac{\lambda_1}{\bar{M}_B^2}\right)$$

$$- 3.96\left(\frac{\lambda_2}{\bar{M}_B^2}\right) + \left|\frac{V_{ub}}{V_{cb}}\right|^2\left(1.33 - 10.3\frac{\bar{\Lambda}}{\bar{M}_B}\right) - 0.4\left(\frac{\bar{\Lambda}}{\bar{M}_B}\right)^3$$

$$- 5.7\left(\frac{\bar{\Lambda}\lambda_1}{\bar{M}_B^3}\right) - 6.8\left(\frac{\bar{\Lambda}\lambda_2}{\bar{M}_B^3}\right) - 7.7\left(\frac{\rho_1}{\bar{M}_B^3}\right) - 1.3\left(\frac{\rho_2}{\bar{M}_B^3}\right)$$

$$- 3.2\left(\frac{\tau_1}{\bar{M}_B^3}\right) - 4.5\left(\frac{\tau_2}{\bar{M}_B^3}\right) - 3.1\left(\frac{\tau_3}{\bar{M}_B^3}\right) - 4.0\left(\frac{\tau_4}{\bar{M}_B^3}\right)$$

$$- \frac{\alpha_s}{\pi}\left(0.035 + 0.07\frac{\bar{\Lambda}}{\bar{M}_B}\right) - 0.082\left(\frac{\alpha_s}{\pi}\right)^2\beta_0. \qquad (16)$$

In Fig. 5 we show the $\Delta\chi^2 = 1$ contours for electrons and muons corresponding to the quoted experimental uncertainties.

The theoretical uncertainties on the HQE parameters are determined by varying, with flat distributions, the input parameters within their respective errors: $|V_{ub}/V_{cb}| = 0.09 \pm 0.02$ [20], $\alpha_s = 0.22 \pm 0.027$, $\lambda_2 = (0.128 \pm 0.010)$ GeV^2 [4], $\rho_2 = 0 \pm (0.5)^3$ GeV^3, and $\tau_i = 0.0 \pm (0.5)^3$ GeV^3 [4]. The parameter ρ_1 is taken as $0.5(0.5)^3 \pm 0.5(0.5)^3$ GeV^3, because it is expected to be positive [7]. The contour that contains 68% of the probability is shown in Fig. 6. This procedure for evaluating the theoretical uncertainty from the unknown expansion parameters that enter at order $1/M_B^3$ is similar to that used by Gremm and Kapustin [4] and Bauer and Trott [9], but is different from the procedure used in our analysis of hadronic mass moments [11]. The dominant theoretical uncertainty is related to the $1/M_B^3$ terms in the nonperturbative expansion discussed before. Reference [21] has explored the convergence of the perturbative and non-
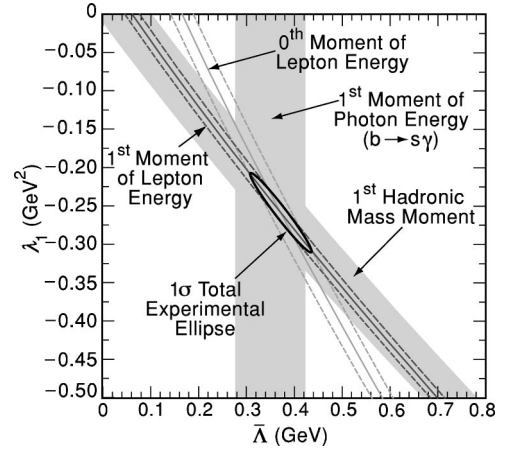
perturbative series appearing in the expressions for the moments described in this paper. The most conservative estimate gives a truncation error of at most 20% of the central values of the HQE parameters. The theoretical uncertainties presented in this paper do not include this truncation error. The measured λ_1 and $\bar{\Lambda}$ are given in Table IV.

A previous CLEO measurement used the first moment of the hadronic recoil mass [11] and the first photon energy moment from the $b \to s\gamma$ process [10]. Figure 7 shows a comparison of our results with the previously published ones. We overlay the experimental ellipse from the electron and muon combined spectral measurement, using in this case $|V_{ub}/V_{cb}| = 0.07$ to be consistent with the assumptions in that paper. The agreement is good, although the theoretical uncertainties do not warrant a very precise comparison.

Using the expression for the full semileptonic decay width given in Eq. (1), we can extract $|V_{cb}|$. We use $\Gamma_{sl}^{exp} = (0.43$
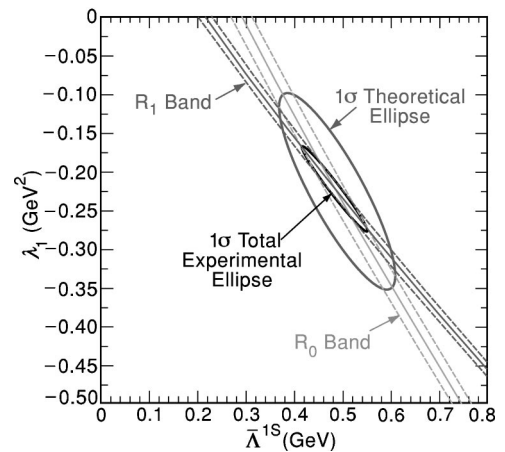

FIG. 8. The combined electron and muon R_0 and R_1 constraints on the parameters $\bar{\Lambda}^{1S}$ and λ_1, showing the $\Delta\chi^2 = 1$ contours for total experimental and theoretical uncertainties, using the constraints in Ref. [9].

TABLE IV. Measured λ_1 and $\bar{\Lambda}$ values, including statistical, systematic, and theoretical errors.

	λ_1 (GeV^2)	$\bar{\Lambda}$ (GeV)
$e^{\pm}$	$-0.28 \pm 0.03_{stat} \pm 0.06_{sys} \pm 0.14_{th}$	$0.41 \pm 0.04_{stat} \pm 0.06_{sys} \pm 0.12_{th}$
$\mu^{\pm}$	$-0.22 \pm 0.04_{stat} \pm 0.07_{sys} \pm 0.14_{th}$	$0.36 \pm 0.06_{stat} \pm 0.08_{sys} \pm 0.12_{th}$
$\ell^{\pm}$	$-0.25 \pm 0.02_{stat} \pm 0.05_{sys} \pm 0.14_{th}$	$0.39 \pm 0.03_{stat} \pm 0.06_{sys} \pm 0.12_{th}$

TABLE V. The measured $\bar{\Lambda}^{1S}$ and m_b^{1S}. The quoted errors reflect statistical, systematic, and theoretical uncertainties, respectively.

	$\bar{\Lambda}^{1S}$ (GeV)	m_b^{1S} (GeV/c^2)	λ_1 (GeV^2)
$e^{\pm}$	$0.52 \pm 0.04_{stat} \pm 0.06_{sys} \pm 0.11_{th}$	$4.79 \pm 0.07_{exp} \pm 0.11_{th}$	$-0.26 \pm 0.03_{stat} \pm 0.05_{sys} \pm 0.12_{th}$
$\mu^{\pm}$	$0.46 \pm 0.05_{stat} \pm 0.08_{sys} \pm 0.11_{th}$	$4.85 \pm 0.07_{exp} \pm 0.11_{th}$	$-0.19 \pm 0.04_{stat} \pm 0.07_{sys} \pm 0.12_{th}$
$\ell^{\pm}$	$0.49 \pm 0.03_{stat} \pm 0.06_{sys} \pm 0.11_{th}$	$4.82 \pm 0.07_{exp} \pm 0.11_{th}$	$-0.23 \pm 0.02_{stat} \pm 0.05_{sys} \pm 0.12_{th}$

TABLE VI. Measured truncated lepton moments $R_{a,b}^{(3)}$ for $e^{\pm}$, $\mu^{\pm}$, and their weighted average.

	$R_a^{(3)}$(GeV$^{-1.3}$)	$R_b^{(3)}$(GeV$^{0.9}$)
$e^{\pm}$	$0.3013 \pm 0.0006_{stat} \pm 0.0005_{sys}$	$2.2632 \pm 0.0029_{stat} \pm 0.0026_{sys}$
$\mu^{\pm}$	$0.3019 \pm 0.0009_{stat} \pm 0.0007_{sys}$	$2.2611 \pm 0.0042_{stat} \pm 0.0020_{sys}$
$\ell^{\pm}$	$0.3016 \pm 0.0005_{stat} \pm 0.0005_{sys}$	$2.2621 \pm 0.0025_{stat} \pm 0.0019_{sys}$

TABLE VII. Measured truncated $R_{a,b}^{(4)}$ moments for $e^{\pm}$, $\mu^{\pm}$, and their weighted average.

	$R_a^{(4)}$ (GeV$^{0.8}$)	$R_b^{(4)}$ (GeV$^{-0.4}$)
$e^{\pm}$	$2.1294 \pm 0.0028_{stat} \pm 0.0027_{sys}$	$0.6831 \pm 0.0005_{stat} \pm 0.0007_{sys}$
$\mu^{\pm}$	$2.1276 \pm 0.0040_{stat} \pm 0.0015_{sys}$	$0.6836 \pm 0.0008_{stat} \pm 0.0014_{sys}$
$\ell^{\pm}$	$2.1285 \pm 0.0024_{stat} \pm 0.0018_{sys}$	$0.6833 \pm 0.0005_{stat} \pm 0.0006_{sys}$

TABLE VIII. Measured duality moments and theoretical predictions using the values λ_1 and $\bar{\Lambda}^{1S}$ reported in this paper. The errors reflect the experimental uncertainties in these parameters and the theoretical errors, respectively.

	Experimental	Theoretical
D_3	$0.5193 \pm 0.0008_{exp}$	$0.5195 \pm 0.0006_{\lambda_1, \bar{\Lambda}^{1S}} \pm 0.0003_{th}$
D_4	$0.6036 \pm 0.0006_{exp}$	$0.6040 \pm 0.0006_{\lambda_1, \bar{\Lambda}^{1S}} \pm 0.0005_{th}$

$\pm 0.01) \times 10^{-10}$ MeV [1]. Assuming the validity of quark-hadron duality, we obtain

$$|V_{cb}| = (40.8 \pm 0.5_{\Gamma_{sl}} \pm 0.4_{\lambda_1, \bar{\Lambda}} \pm 0.9_{th}) \times 10^{-3}, \quad (17)$$

where the first uncertainty is from the experimental value of the semileptonic width, the second uncertainty is from the HQE parameters (λ_1 and $\bar{\Lambda}$), and the third uncertainty is the theoretical uncertainty obtained as described above.

B. Determination of the short range mass m_b^{1S}

We use the formalism of Ref. [9] to extract the short range mass of the b quark m_b^{1S}, defined as $m_b^{1S} \equiv \bar{M}_B - \bar{\Lambda}^{1S}$. Table V summarizes the measurement of $\bar{\Lambda}^{1S}$ and λ_1 for electrons and muons separately, and for the combined sample. Figure 8 shows the corresponding bands and the $\delta\chi^2 = 1$ contour. The theoretical uncertainty is extracted using the method described above. Our result, $m_b^{1S} = (4.82 \pm 0.07_{exp} \pm 0.11_{th})$ GeV/c^2, is in good agreement with a previous estimate of m_b^{1S} [13] derived from $\Upsilon(1S)$ data, $m_b^{1S} = 4.69 \pm 0.03$ GeV/c^2.

C. Measurements of additional spectral moments and implications for the HQE parameters

We apply the same experimental procedure described before to measure a variety of spectral moments. In particular, we measure the moments $R_a^{(3)}$, $R_b^{(3)}$, $R_a^{(4)}$, and $R_b^{(4)}$ defined in Eqs. (8)–(11). Tables VI and VII summarize their measured values, as well as the statistical and systematic errors. Figure 9 shows the measured $\bar{\Lambda}^{1S}$ and λ_1 with these two sets of constraints, as well as the constraints derived from the moments R_0 and R_1. Although we are able to confirm that $1/M_B^3$ terms produce much smaller uncertainties using $R_{a,b}^{(3,4)}$, the experimental errors are larger in this case because of the similar slopes for the two constraints. The uncertainty ellipses are still sizable, but the systematic and theoretical uncertainties have a different nature and magnitude and thus the overall agreement is significant.

Finally, we extract the duality moments D_3 and D_4 from the measured shape of the electron and muon spectra. The theoretical predictions for these moments in Ref. [9], evaluated using the values of $\bar{\Lambda}^{1S}$ and λ_1 reported in this paper, are compared with the measured $D_{3,4}$ from the combined lepton sample in Table VIII. The agreement is excellent and
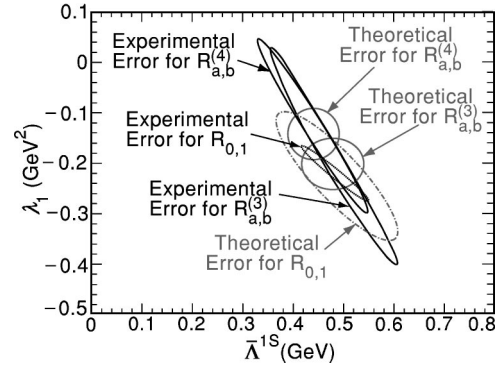

FIG. 9. Constraints on the HQE parameters λ_1 and $\bar{\Lambda}^{1S}$ from all our measured spectral moments.

thus no internal inconsistency of the theory is uncovered in this analysis.

IV. CONCLUSION

We have measured the lepton momentum spectra in $\bar{B} \to X \ell \bar{\nu}$ ($\ell = e$ and μ) for $p \geq 1.5$ GeV/c in the B rest frame. From these, we determine the spectral moments R_0, R_1, $R_a^{(3)}$, $R_b^{(3)}$, $R_a^{(4)}$, $R_b^{(4)}$, D_3 and D_4.

Using the moments R_0 and R_1 we extract the HQE parameters $\bar{\Lambda} = (0.39 \pm 0.03_{stat} \pm 0.06_{sys} \pm 0.12_{th})$ GeV and $\lambda_1 = (-0.25 \pm 0.02_{stat} \pm 0.05_{sys} \pm 0.14_{th})$ GeV^2. These results imply that the pole mass $m_b = (4.90 \pm 0.08_{exp} \pm 0.13_{th})$ GeV/c^2. The short range mass m_b^{1S} is found to be $(4.82 \pm 0.07_{exp} \pm 0.11_{th})$ GeV/c^2. We obtain $|V_{cb}| = (40.8 \pm 0.5_{\Gamma_{sl}} \pm 0.4_{\lambda_1, \bar{\Lambda}} \pm 0.9_{th}) \times 10^{-3}$, without any quantified error associated with the assumption of quark-hadron duality.

Finally, an extensive study of different spectral moments shows good agreement between independent determinations of the HQE parameters.

[1] M. Artuso and E. Barberio, in Particle Data Group, K. Hagiwara *et al.*, Phys. Rev. D **66**, 010001 (2002); hep-ph/0205163.

[2] A.V. Manohar and M.B. Wise, Phys. Rev. D **49**, 1310 (1994).

[3] I. Bigi, M.A. Shifman, N.G. Uraltsev, and A. Vainshtein, Phys. Rev. Lett. **71**, 496 (1993).

[4] M. Gremm and A. Kapustin, Phys. Rev. D **55**, 6924 (1997).

[5] M. Gremm and I. Stewart, Phys. Rev. D **55**, 1226 (1997).

[6] I. Bigi, N.G. Uraltsev, and A. Vainshtein, Phys. Lett. B **293**,

430 (1992); **297**, 477(E) (1993); M. Jezabeck and J.H. Kühn, Nucl. Phys. **B314**, 1 (1989); M. Luke, M.J. Savage, and M.B. Wise, Phys. Lett. B **345**, 301 (1995).

[7] M.A. Shifman and M.B. Voloshin, Sov. J. Nucl. Phys. **45**, 292 (1987); V.A. Khoze, M.A. Shifman, N.G. Uraltsev, and M.B. Voloshin, *ibid.* **46**, 112 (1987).

[8] M. Gremm, A. Kapustin, Z. Ligeti, and M. Wise, Phys. Rev. Lett. **77**, 20 (1996).

[9] C. Bauer and M. Trott, Phys. Rev. D **67**, 014021 (2003).

[10] CLEO Collaboration, S. Chen *et al.* Phys. Rev. Lett. **87**, 251807 (2001).

[11] CLEO Collaboration, D. Cronin-Hennessy *et al.* Phys. Rev. Lett. **87**, 251808 (2001).

[12] I.I. Bigi, M. Shifman, N. Uraltsev, and A.I. Vainshtein, Phys. Rev. D **50**, 2234 (1994).

[13] A.H. Hoang, Phys. Rev. D **61**, 034005 (2000); Nucl. Phys. B (Proc. Suppl.) **86**, 512 (2000); A.H. Hoang and A.V. Manohar, Phys. Lett. B **483**, 94 (2000); A.H. Hoang, CERN-TH/2000-227, hep-ph/0008102; A.H. Hoang, CERH-TH/2001-48, hep-ph/0102292.

[14] A.X. El-Khadra and M.L. Luke, Ann. Rev. Nucl. Sci. **52**, 201

[15] BaBar Collaboration, B. Aubert *et al.*, hep-ex/0207084.

[16] DELPHI Collaboration, Contributed Paper, ICHEP02,2002-0070-CONF-604, and 2002-0071-CONF-605; M. Battaglia *et al.*, J. High Energy Phys. **12**, 004 (2002).

[17] CLEO Collaboration, Y. Kubota *et al.*, Nucl. Instrum. Methods Phys. Res. A **320**, 66 (1992).

[18] D. Atwood and W. Marciano, Phys. Rev. D **41**, 1736 (1990).

[19] E. Barberio and Z. Wąs, Comput. Phys. Commun. **79**, 291 (1994).

[20] A. Falk, Nucl. Phys. B (Proc. Suppl.) **111**, 3 (2002).

[21] C. Bauer, Z. Ligeti, M. Luke, M.B. Wise, and A.V. Manohar, Phys. Rev. D **67**, 054012 (2003).

(2002); hep-ph/0208114.